Extended Abstracts of the 2013 International Conference on Solid State Devices and Materials, Fukuoka, 2013, pp436-437

Nonequilibrium Green Function Simulations of Graphene-Nanoribbon Resonant-Tunneling Transistors

N. Mori[1,2,†], T. Edagawa[1], Y. Kamakura[1,2], and L. Eaves[3]

[1]*Graduate School of Engineering, Osaka University, 2-1 Yamada-oka, Suita, Osaka 565-0871, Japan*
[2]*CREST, JST, 5 Sanbancho, Chiyoda-ku, Tokyo 102-0075, Japan*
[3]*School of Physics & Astronomy, University of Nottingham, Nottingham NG7 2RD, United Kingdom*
[†]*E-mail: mori@physics.org*

Strong negative differential conductance (NDC) was reported recently in graphene/hexagonal-boron-nitride (hBN) resonant-tunneling transistors (RTTs) [1]. These devices have potential for future high-frequency and logic applications. Here we use Green function calculations to study the effect on the electronic characteristics of reducing the device dimensions down to the nanometer scale. Nanoscale confinement is known to strongly modify the properties of conventional resonant tunneling devices [2].

Figure 1 shows a schematic diagram of the graphene-nanoribbon (GNR) RTT considered in the present study. Our structure is the same as that in ref. [1] except that the active region consists of a ultrathin ribbon only a few nm in width. We focus on the metallic armchair edge GNR whose width $W = (M - \frac{1}{2})3a_0$ with $M = 4, 7, 10, \ldots$, and where a_0 is the graphene lattice constant. The channel length is $L = (N - \frac{1}{4})\sqrt{3}a_0$ (see the inset of Fig. 4).

We calculate the current-voltage characteristics using the nonequilibrium Green function (NEGF) method combined with a tight-binding approximation in the ballistic limit (no scattering). We first extract the tight-binding parameters describing the bandstructure of graphene/(hBN)$_n$/graphene systems ($n = 1, 2, 3, 4$) from first-principles calculations (see Fig. 2). The source-drain current, I, is then determined as a function of drain voltage, V_d, at fixed gate bias, V_g. The applied voltages are converted to internal potential energies using a simple capacitance model, see Fig. 3.

Figure 4 shows I–V_d characteristics of the GNR/(hBN)$_2$ RTT with $W = 0.9$ nm ($M = 4$) and $L = 100$ nm ($N = 235$) at $T = 300$ K. The nanoribbon width is so small that higher subbands move away from the Dirac point (see Fig. 5) and do not contribute to the current. The current-voltage characteristics resemble those observed in the graphene-based RTTs [1] except for a weak oscillatory structure, due to carrier reflection at the channel boundaries along the source-to-drain direction. In the I–V_d curves, a pronounced peak occurs in the current, whose amplitude and drain-voltage position depends on gate bias. Note that these calculations do not include the effects of the residual doping and the peak position is essentially symmetric with respect to V_g.

For a wider nanoribbon, higher subbands also contribute to the current. Figure 6 shows the I–V_d characteristics of the GNR/(hBN)$_2$ RTT with $W = 5.3$ nm ($M = 22$) and $L = 100$ nm ($N = 235$) at $T = 300$ K. Due to inter-subband transitions, two types of structure appear in addition to the main peak: broad structures [e.g. onsets labeled (a) and (e) on I–V_d at $V_\mathrm{g} = -2$ V] and sharp structures [peaks (b), (d), and (f)]. The latter originate from the resonance at $k = 0$ [see Fig. 7 (b), (d), and (f)], while the former are due to the resonance at finite k [see Fig. 7(a) and (e)].

Our analysis indicates that nanoscale confinement does not destroy the resonant peaks and NDC of graphene RTTs; indeed, it could be exploited to fine-tune the device characteristics.

[1] L. Britnell *et al.*, Nat. Commun. **4**, 1794 (2013).
[2] P. H. Beton *et al.*, Phys. Rev. Lett. **75**, 1996 (1995).

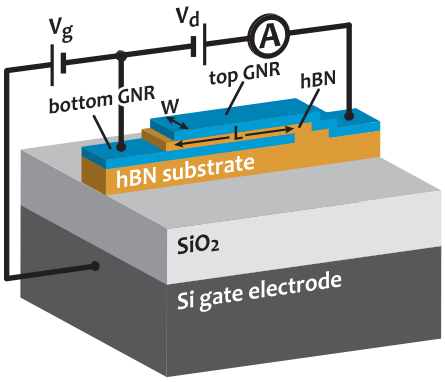

Figure 1: Schematic diagram of the GNR/hBN resonant-tunneling transistor.

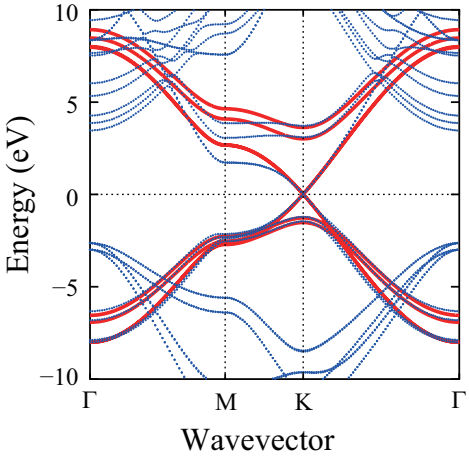

Figure 2: Band-structures of graphene/(hBN)$_2$/graphene calculated by the first-principles (blue thin dotted line) and the tight-binding approximation (red thick solid line).

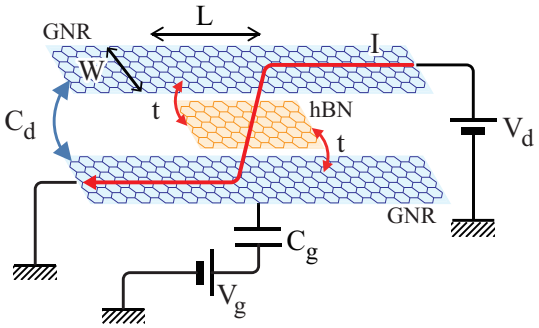

Figure 3: Schematic diagram of the device model used for the NEGF simulation.

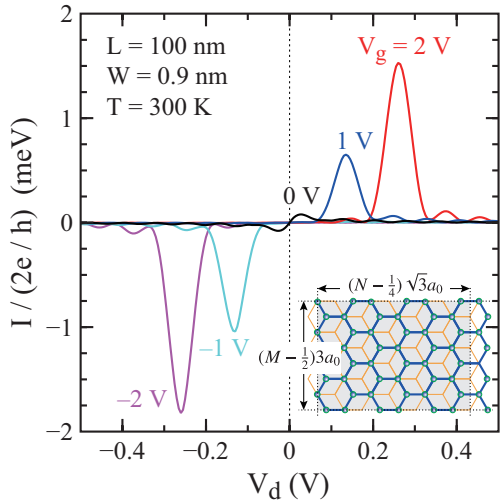

Figure 4: Current-voltage characteristics at 300 K for a narrow device of W = 0.9 nm (M = 4). Inset shows the schematics of the stacking arrangement.

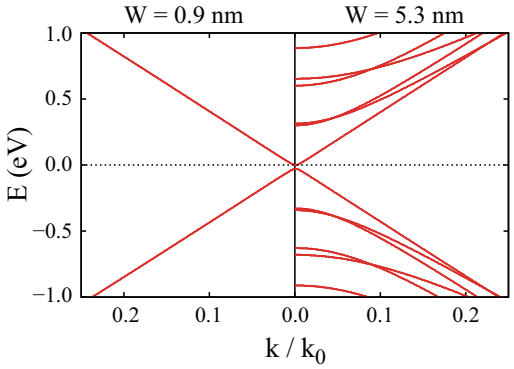

Figure 5: Band-structures of GNR/(hBN)$_2$/GNR with$W$ = 0.9 nm (left panel) and W = 5.3 nm (right panel); k is along the ribbon axis.

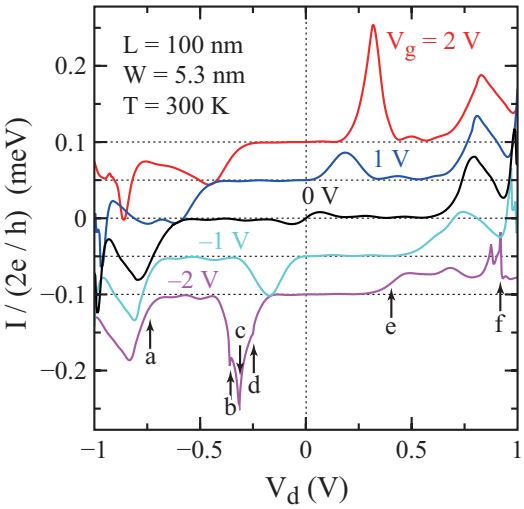

Figure 6: Current-voltage characteristics at 300 K for a wide device of W = 5.3 nm (M = 22). Curves are vertically offset for clarity.

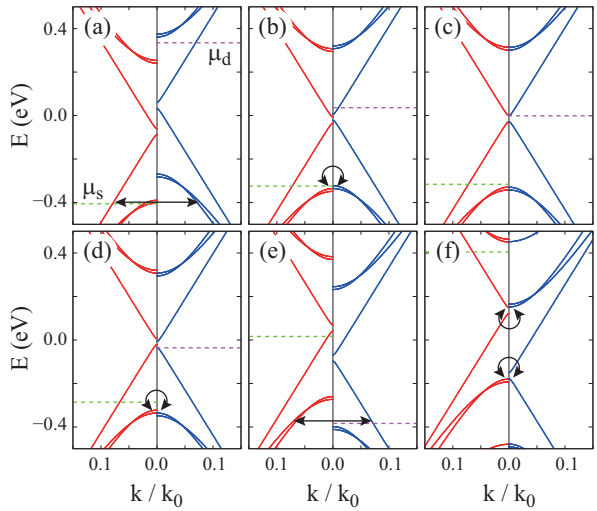

Figure 7: Band alignment at the bias conditions labeled (a)-(f) in Fig. 6. Arrows represent the inter subband transition.